Transgenerational sterility of Piwi pathway mutants in response to germ granule dysfunction

Short title: Germ granules orchestrate Piwi sterility

Authors: Katherine Kretovich Billmyre[1,2]†, Bree Heestand[1,2,3]†, Maya Spichal[1,2]†, Stephen Frenk[1,2]† and Shawn Ahmed[1,2,3*]

Affiliations:

[1]Department of Genetics, University of North Carolina, Chapel Hill, NC, USA

[2]Department of Biology, University of North Carolina, Chapel Hill, NC, USA

[3]Lineberger Comprehensive Cancer Center, University of North Carolina, Chapel Hill, NC, USA

†These authors contributed equally to this manuscript

*Corresponding author: shawn@med.unc.edu

Abstract:

Germ cells deficient for Piwi and associated small RNA genome silencing factors transmit a form of heritable stress that induces sterility after growth for several generations. The cause of this transgenerational sterility phenotype is not understood but has been attributed to progressive deterioration of heterochromatin and associated DNA damage. Sterile small RNA genome silencing mutants displayed inconsistent increases in DNA damage signaling but consistently altered perinuclear germ granules. Germ granule dysfunction was sufficient to induce phenotypes associated with sterile small RNA genome silencing mutants, including germline atrophy, reproductive diapause and univalents in oocytes. Genes that perturb germ granule structure were not compromised in sterile small RNA mutants, suggesting a post-transcriptional reproductive arrest mechanism. We conclude that the integrity of germ granules, which are intimately associated with Piwi silencing factors, orchestrates the sterility of Piwi deficient mutants and could be generally relevant to regulation of reproductive arrest in response to stress.

Significance Statement:

Sterility in response to heterochromatin dysfunction was recognized in *Drosophila* P-M Hybrid Dysgenesis experiments carried out by Margaret Kidwell in the 1970's and more recently in mutants deficient for Piwi/piRNA silencing. A central model of these studies is that this sterility is caused by transposon expression and associated genomic instability. We demonstrate that sterility in response to deficiency for Piwi is a form of reproductive arrest that is orchestrated by germ granule dysfunction. Germ granules

promote genomic silencing of transposons and viruses, and they are likely to be frequently targeted by these parasites. We hypothesize the evolution of a reproductive arrest mechanism that responds to attacks on germ granules by disrupting their integrity.

Keywords: Germ granules, reproductive arrest, small RNAs, heterochromatin, germ cell immortality, Heritable Stress, Piwi

Introduction:

Germ cells give rise to the mortal somatic tissues while maintaining themselves in a pristine condition that allows them to be propagated for an indefinite number of generations. This capacity for self-renewal is termed “germ cell immortality”, and functions to protect the germline from forms of damage that can result in sterility (Smelick and Ahmed, 2005). Defects in *Caenorhabditis elegans* (*C. elegans)* genes that promote small RNA-mediated genome silencing (Fig. 5a) can cause a Mortal Germline *(mrt)* phenotype, where robust fertility occurs for several generations but deteriorates in later generations, finally culminating in complete sterility. Many *mrt* mutants only become sterile when grown at the non-permissive temperature 25˚C (Ahmed and Hodgkin, 2000), some of which are deficient for small RNA-mediated genome silencing (Ashe et al., 2012; Buckley et al., 2012; Burkhart et al., 2011; McMurchy et al., 2017; Sakaguchi et al., 2014; Smelick and Ahmed, 2005; Spracklin et al., 2017). However, the piRNA-deficient mutant *prg-1* and the nuclear RNA interference (RNAi) mutants *nrde-1* and *nrde-4* display progressive sterility at any temperature (Batista et al., 2008; Buckley

et al., 2012; Burkhart et al., 2011; Das et al., 2008; McMurchy et al., 2017; Simon et al., 2014).

Piwi is a conserved germ line Argonaute protein that interacts with thousands of small RNAs termed piRNAs to repress transposons and foreign nucleic acids that represent parasitic threats to the integrity of the genome (Aravin et al., 2007; Luteijn and Ketting, 2013; Siomi et al., 2011). Deficiency for the *C. elegans* Piwi ortholog *prg-1* compromises germ cell immortality, and late-generation *prg-1* mutant strains were recently shown to elicit a striking germ cell atrophy phenotype at the generation of sterility, as L4 larvae mature into 1 day old adults (Heestand et al., 2018). Moreover, atrophied germ lines of sterile *prg-1* mutants can regrow on day 2 of adulthood, and a small fraction of constitutively sterile 5 day old *prg-1* mutant adults can become fertile again if they are shifted to a distinct food source (Heestand et al., 2018). This indicates that the late-generation sterility of *prg-1*/Piwi mutants is a form of reproductive arrest termed Adult Reproductive Diapause, which can be induced in response to environmental stresses such as starvation (Angelo and Van Gilst, 2009; Padilla and Ladage, 2012; Tatar and Yin, 2001). We therefore proposed that late-generation sterility of *prg-1*/Piwi mutants may occur in response to accumulation of a heritable stress that is transmitted by germ cells (Heestand et al., 2018). Consistently, temperature-sensitive small RNA genome silencing mutants *rsd-2* and *rsd-6* also exhibit small and empty germlines at the generation of sterility (Sakaguchi et al., 2014).

Transposon-induced genome instability has been implicated in the acute sterility phenotype of Piwi/piRNA mutants in several species (Juliano et al., 2011; Siomi et al., 2011), and fertility defects in response to heterochromatin dysfunction have been

92 associated with increased levels of RNA-DNA hybrids and of transposon-induced DNA
93 damage (McMurchy et al., 2017; Zeller et al., 2016). *C. elegans prg-1* mutants display
94 progressively increased levels of germline apoptosis when grown for successive
95 generations, and apoptosis promotes germ cell atrophy for sterile *rsd-2*, *rsd-6* and *prg-1*
96 mutants (Heestand et al., 2018; Sakaguchi et al., 2014; Simon et al., 2014). Given that
97 very low levels of transposition occur in late-generation *prg-1* mutants (Simon et al.,
98 2014), and given that the transgenerational sterility phenotype of small RNA-mediated
99 genome silencing mutants is reversible (Heestand et al., 2018; Simon et al., 2014;
100 Spracklin et al., 2017), their sterility is unlikely to be a consequence of debilitating levels
101 of transposon-induced DNA damage. Finally, high levels of transposition occur in *C.*
102 *elegans mutator* mutants but this is not sufficient to induce transgenerational sterility at
103 permissive temperature (Simon et al., 2014).

104 Another proposed cause of sterility in *C. elegans* small RNA genome silencing
105 mutants is misrouting of small RNAs that regulate the epigenome (de Albuquerque et
106 al., 2015; Phillips et al., 2015). Some Argonaute proteins that regulate epigenomic
107 pathways are located in perinuclear germ granules, which are conserved germline
108 structures akin to liquid droplets that interact with nuclear pore complexes and are
109 necessary for fertility (Updike et al., 2011). *C. elegans* germ granules are termed P
110 granules based on antibodies that label the P blastomere that generates the germ cell
111 lineage (Strome and Wood, 1982). Core P granule proteins have been shown to play
112 redundant functions making it difficult to eliminate P granules (Updike et al., 2014). Here
113 we study the late-generation sterility phenotype of small RNA-mediated genome
114 silencing mutants and find that it is linked to dysfunction of P granules, a mechanism

115 that could be generally relevant to the regulation of stress-induced reproductive arrest
116 and to the long-standing observation that desilencing of heterochromatin can induce
117 sterility.
118
119 **Results:**
120 **Genome instability in small RNA mutants**
121 Transgenerational sterility in *C. elegans* telomerase mutants that lack the ability to
122 maintain sequences that cap chromosome ends is caused by high levels of telomere
123 fusions and associated genome damage (Ahmed and Hodgkin, 2000). We examined
124 *prg-1* mutants grown at 20°C across several generations for the presence of the DNA
125 damage response, as detected by an antibody to phosphorylated S/TQ, a protein
126 modification that is created by two sensors of DNA damage, the phosphatadylisonisol-3-
127 kinase like protein kinases ATM and ATR (Kim et al., 1999; Vermezovic et al., 2012).
128 We observed a significant increase in the fraction of germ cells with upregulated DNA
129 damage response for late-generation fertile *prg-1* mutants (~3-fold) and sterile *prg-1*
130 mutants (~6-fold) when compared to either wild-type controls or to early-generation *prg-*
131 *1* mutants (Fig. 1a,b). We also tested temperature-sensitive small RNA mutants and
132 found that the wild-type DNA damage response was upregulated in many cells by
133 growth at 25°C but that this level did not change in sterile *rsd-6, nrde-2* or *hrde-1* mutant
134 germlines (Fig. 1b,c). Therefore, although the DNA damage response is induced in late-
135 generation *prg-1* mutants, it is not consistently altered in sterile small RNA genome
136 silencing mutants.
137

138 **Small RNA mutants exhibit P- granule defects at sterility**

139 Deficiency for PRG-1 causes delocalization of the P granule protein PGL-1 (Phillips et
140 al., 2015), and combined loss of the epigenomic regulators SPR-5 and LET-418, or loss
141 of H3K9 methylation modifier SET-2 and the nuclear RNAi pathway, results in
142 immediate sterility that is associated with disruption of P granules (Käser-Pébernard et
143 al., 2014; Robert et al., 2014). Whilst characterizing germ line defects of sterile *rsd-6*
144 mutants by immunofluorescence, we found that a P granule antibody exhibited altered
145 staining patterns in sterile but not fertile late-generation *rsd-6* mutant siblings (Fig 2d-d').
146 We also found that sterile late-generation *hrde-1* and *nrde-2* temperature-sensitive
147 mutant germ lines displayed P granule defects (Fig 2c-c', S1), which were absent or
148 comparatively minor in fertile late-generation mutants that were close to the generation
149 of sterility (Fig. 2c-c', S1, Table 1). When compared to wild-type controls, P granule
150 dysfunction in the sterile mutants ranged from a loss of P granules in a subset of cells to
151 varying amounts of P granule disorganization (Fig. 2, S1). Sterile *hrde-1(tm200)* mutant
152 animals displayed the most severe P granule phenotype, as the majority of sterile *hrde-*
153 *1* mutant germ cells exhibited little to no staining (Fig. S1). We also examined the
154 temperature sensitive *mrt* mutant *rbr-2(tm1231)*, which encodes a histone 3 lysine 4
155 demethylase that promotes genomic silencing and likely functions downstream of small
156 RNAs to promote germ cell immortality (Alvares et al., 2014). Similarly to *hrde-1* and
157 *nrde-2*, late generation fertile *rbr-2* animals did not exhibit obvious P granule defects,
158 while loss of P granules was observed in many germ cells at sterility (Fig. 2e-e').

159 Germ line atrophy occurs in some but not all *prg-1* mutants as L4 larvae develop
160 into sterile adults (Heestand et al., 2018). Large-scale apoptosis contributes to this germ

161 cell degeneration phenotype (Heestand et al., 2018), and P granules have been shown
162 to vanish in cells that undergo apoptosis (Min et al., 2016; Sung et al., 2017). However,
163 we observed widespread P granule dysfunction in sterile germlines of *rsd-6* mutants
164 that were wildtype in size and had not undergone significant amounts of apoptosis (Fig.
165 2d).

166 *nrde-1* and *nrde-4* animals displayed a distinct phenotype, whereby only a
167 subpopulation displayed P granule defects (60% and 22% respectively (Fig. S1, Table
168 S1)). This suggests that loss of *nrde-1* and *nrde-4*, which act downstream of multiple
169 small RNA (and possibly other epigenetic) pathways, may lead to sterility via several
170 distinct mechanisms.

171 In contrast to most small RNA genome silencing mutants where fertility defects
172 are not severe until the generation of sterility, late-generation *prg-1* mutants display very
173 small brood sizes for many generations prior to sterility (Heestand et al., 2018). By
174 immunofluorescence, we observed a wide range of P granule defects that could be
175 identified in both sterile and fertile late-generation *prg-1* mutant germ cells (Fig. 2b, S1).
176 Many germlines exhibited strong P granule dysfunction that either resulted in a total
177 absence of or an irregular distribution of P granules (Fig. 2b-b', S1).

178 *C. elegans* P granules are adjacent to Mutator bodies, which house Mutator
179 proteins that amplify primary siRNA populations into secondary effector siRNAs via
180 RNA-dependent RNA polymerase (Phillips et al., 2012). *mutator* mutants are
181 dysfunctional for of secondary siRNAs and remain fertile indefinitely at low temperatures
182 (Simon et al., 2014), but display an immediate highly penetrant sterility phenotype at
183 25°C that could be caused by dysfunction of small RNA-mediated heterochromatin

184 (Ketting et al., 1999). We examined sterile *mut-14* mutants at the restrictive
185 temperatures 25°C and observed pronounced P granule defects in 87% of animals (Fig.
186 2f-f', Table 1).
187

188 **P granule dysfunction is sufficient to elicit phenotypes of sterile small RNA**
189 **silencing mutants**

190 We initially addressed the significance of P granule dysfunction in sterile late-generation
191 small RNA genome silencing mutants using an RNA interference clone that
192 simultaneously targets four P granule subunits *pgl-1*, *pgl-3*, *glh-1*, *glh-4* (Knutson et al.,
193 2017; Updike et al., 2014). This resulted in many F2 sterile adults at 25˚C (80%) (Fig.
194 3a). The germlines of F2 P granule RNAi L4 larvae were normal in size in comparison to
195 control worms. However, a pronounced germ cell atrophy phenotype occurred as many
196 P granule-depleted animals matured into sterile adults, resulting in a significant change
197 in their germline profile (Fig. 3b, p=3.93E-24). Furthermore, oocyte univalents were
198 previously observed in sterile but not fertile late-generation *rsd-6* mutants (Sakaguchi et
199 al., 2014), and 45.5% of oocytes of sterile P granule depleted adults contained 7-12
200 univalents (Fig. 3c, e-h).
201

202 **Deficiency for *pgl-1* phenocopies of reproductive arrest of sterile *prg-1* mutants**

203 We considered that the germline atrophy phenotypes observed in P granule-depleted
204 worms might mimic the Adult Reproductive Diapause phenotype of sterile *prg-1* mutant
205 adults, which can regrow their atrophied germlines and become fertile (Heestand et al.,
206 2018). To test this hypothesis, we used a mutant deficient for the P granule component

207 *pgl-1*, which displays a pronounced sterility phenotype if shifted to the restrictive
208 temperature of 25°C (Kawasaki et al., 1998). While most first generation F1 *pgl-1*
209 animals at 25°C displayed normal germlines at the L4 larval stage, there was a
210 significant shift in the germline profiles with 52% of day 1 adults showing germline
211 atrophy (Fig. 3b) (p=1.04E-35), similar to P granule RNAi knockdown and sterile *prg-1*
212 mutants (Heestand et al., 2018). Furthermore, when oocytes of sterile *pgl-1* mutant
213 adults were scored, we found that 56.7% of oocytes had univalents, in agreement with
214 the oocyte univalents observed in response to P granule depletion by RNAi (Fig. 3c).
215 At 25°C, some F1 *pgl-1* mutants were fertile and gave rise to maternally depleted
216 F2 animals that were uniformly sterile. F2 L4 larvae had germline profiles that displayed
217 more severe germ cell proliferation defects than those of F1 L4 larvae, and day 1 adults
218 showed a striking 54% increase in empty germlines (Fig. 3d) (p=2.44E-05). Therefore,
219 germlines of F1 progeny of *pgl-1* mutant mothers that were shifted to the restrictive
220 temperature mimicked the germ cell degeneration phenotypes of sterile small RNA
221 genome silencing mutants as L4 larvae matured into adults, whereas F2 generation *pgl-*
222 *1* mutant larvae displayed more pronounced germ cell proliferation defects.
223 We asked if the fertility of sterile 25°C F1 *pgl-1* mutants could be restored by
224 shifting them to the permissive temperature of 20°C. Sterile F1 *pgl-1* mutants that
225 lacked embryos were shifted to 20°C on day 1 of adulthood and their germlines were
226 scored after 48 hours, which revealed a significant change in their germline profiles
227 (p=0.007), with a shift from atrophied germlines towards large germlines when
228 compared to sterile F1 *pgl-1* sibling controls that remained sterile at 25°C (Fig. 3i). In
229 agreement with this amelioration of germline size, we observed that some sterile F1 *pgl-*

230 *1* mutant adults that were shifted to 20°C for several days had laid oocytes and dead
231 embryos, and that a few even gave rise to progeny (Fig. 3j). In contrast, sterile *pgl-1*
232 mutant control adults that were kept at 25°C never gave rise to oocytes, dead embryos
233 or living progeny (Fig. 3j). The frequency of fertility observed in this circumstance is very
234 similar to sterile *prg-1* mutant adults that exit Adult Reproductive Diapause in response
235 to an alternative food source (Heestand et al., 2018). These results indicate that P
236 granule dysfunction could induce Adult Reproductive Diapause, a transient and
237 potentially adaptive form of reproductive arrest.
238

239 **Transcriptional consequences of germ granule dysfunction and small RNA**
240 **genome silencing mutant sterility**

241 The sterility of Piwi/piRNA mutants is thought to result in upregulated expression of
242 transposons and associated genome instability (Heestand et al., 2018). In an effort to
243 deduce how germ granule dysfunction might occur in small RNA genome silencing
244 mutants, we sequenced RNA from the nuclear RNAi defective mutants *nrde-1*, *nrde-2*
245 and *nrde-4*. These mutants are all defective in nuclear silencing in response to
246 exogenous dsRNA triggers (Buckley et al., 2012; Guang et al., 2010, 2008), and at
247 25°C they all have Mortal Germlines (Burkhart et al., 2011). However, at 20°C *nrde-1*
248 and *nrde-4* mutants become progressively sterile but *nrde-2* mutants remain fertile
249 indefinitely (Burkhart et al., 2011). We focused on *nrde-1* and *nrde-4* mutants because
250 they have relatively large brood sizes at sterility at 20°C, such that large cohorts of L4
251 larvae that are poised to become sterile can be collected. In contrast, *prg-1* mutants
252 develop very low brood sizes in late generations (Heestand et al., 2018), and it is

253 difficult to obtain large numbers of synchronous animals that are poised to become
254 sterile. We therefore prepared RNA from early-generation and sterile-generation *nrde-1*
255 and *nrde-4* mutants at 20°C and compared this with RNA from wildtype and *nrde-2*
256 mutant controls.

257 We found that sterile generation *nrde-1* and *nrde-4* mutant L4 larvae showed
258 strong upregulation of similar transposon classes in comparison to early generation
259 *nrde-1* or *nrde-4* mutant L4 larvae or to wildtype controls (Fig. 4a). We identified 18
260 transposon classes that were upregulated at least two-fold in both *nrde-1* and *nrde-4*,
261 13 of which were CER retrotransposons, which is consistent with previous
262 transgenerational analysis of *hrde-1* mutants (Ni et al., 2016). However, we found that
263 *nrde-2* mutant controls that do not become sterile at 20°C displayed strong upregulation
264 of similar transposon loci, even in early generations. Of the 18 transposons upregulated
265 in both *nrde-1* and *nrde-4*, 17 were also upregulated in *nrde-2* compared with wildtype.
266 As a comparison, we analyzed published RNA-seq data from *prg-1(n4357)* mutant
267 animals (McMurchy et al., 2017). Previous papers have reported that distinct classes of
268 transposons are upregulated in *prg-1* and *nrde-2* mutants (Das et al., 2008; McMurchy
269 et al., 2017; Ni et al., 2016; Simon et al., 2014), and we confirmed this result by showing
270 that MIRAGE1 was the only transposon upregulated in both *nrde-1*, *nrde-4* and *prg-1*
271 mutants (Fig. 4a).

272 We compared gene expression data from sterile generation *nrde-1* or *nrde-4*
273 mutant L4 larvae with late-generation *prg-1* mutants (McMurchy et al., 2017) and
274 compared this with RNA from wildtype or *nrde-2* mutant control L4 larvae in order to
275 identify common genes whose expression is specifically induced in L4 larvae that are

276 poised to become sterile and that might explain the P granule abnormalities at sterility.
277 Late-generation *prg-1* mutant and sterile generation *nrde-1* and *nrde-4* mutant gene
278 expression was very different from wildtype or *nrde-2* mutant controls RNA.
279 Spermatogenic genes were over-represented among genes significantly upregulated in
280 sterile generation *nrde-1* and *nrde-4* mutant larvae (p = 1e-15, Chi Square test for both
281 mutants), which is consistent with what has been previously reported for *spr-5* mutants
282 that become progressively sterile (Katz et al., 2009). However, there was no general
283 tendency of an up- or down-regulation of any gene category for *prg-1*, *nrde-1* and *nrde-*
284 *4* mutants. Only 11 genes were significantly upregulated in all three mutants, and there
285 were no commonly downregulated genes (Fig. 4c). We identified a set of 20 genes that
286 were significantly upregulated at least fourfold in *prg-1* and either *nrde-1* or *nrde-4*.
287 which included many *pud* (protein upregulated in dauer) genes that could be an
288 indicator for genes upregulated due to a general stress response of the organism (Table
289 S2). This may be consistent with our recent observation that DAF-16, which promotes
290 dauer formation, is responsible for several phenotypes of sterile generation *prg-1*
291 mutant adults, including germ cell atrophy (Heestand et al., 2018).
292 Knockdown of a number of genes has been shown to disrupt P granule structure
293 in a manner that could be similar to what we observe in sterile small RNA mutant adults
294 (Updike and Strome, 2010). We compared the expression of genes known to perturb P
295 granule structure with genes whose expression is significantly altered in late-generation
296 *prg-1* mutants or in sterile generation *nrde-1* and *nrde-4* mutant L4 larvae. We could find
297 no consistent changes in P granule associated genes in any of the mutants tested.

298 RNA-seq data sets have been previously obtained for germlines of P granule
299 defective L4 larvae and adults (Knutson et al., 2017). In P granule defective adults,
300 somatic genes are overexpressed because these animals display a germline to soma
301 transformation, but germlines of L4 larvae were not significantly different from wildtype.
302 We compared sterile generation *nrde-1* and *nrde-4* RNA from L4 larvae with RNA from
303 germlines of P granule defective L4 larvae (Knutson et al., 2017) and found no genes
304 that were up or downregulated in both *nrde-1/nrde-4* and P granule defective larvae.
305 Moreover, only two out of the 18 transposons upregulated in *nrde-1/nrde-4* were also
306 upregulated in P granule defective L4 larvae (Fig. 4a). We conclude that L4 larvae that
307 are poised to enter reproductive arrest as a consequence of P granule dysfunction do
308 not display a consistent transcriptional signature, nor does P granule dysfunction cause
309 immediate overt effects on expression of heterochromatic segments of the genome.
310 Our analyses indicate that *prg-1* and *nrde-1/nrde-4* have fundamentally different
311 gene expression profiles at or near sterility. We conclude that the sterility phenotype of
312 *prg-1* and *nrde-1/nrde-4* is physiologically similar but very different on a molecular level.
313 Therefore, although deficiency for *prg-1* and *nrde-1/nrde-4* disrupts small RNA-
314 mediated genome silencing and compromises germ cell immortality, these genes have
315 distinct functions with regards to small RNA regulation of the genome such that we
316 observed only a small number of overlapping transcriptional effects. These
317 transcriptional differences could contribute to the more pronounced P granule defects in
318 late-generation *prg-1* mutant germ lines in comparison to the relatively mild effects on P
319 granules in sterile *nrde-1* and *nrde-4* mutants.
320

321 **Discussion:**

322 P-M Hybrid Dysgenesis is a temperature-sensitive *Drosophila* fertility defect that was
323 discovered in the 1970's, where defects in transposon silencing were linked to
324 reproductive failure (Kelleher, 2016; Kidwell et al., 1977). In these experiments,
325 Drosophila M strain females were mated with males of the more recently isolated P
326 strain to yield F1 hybrid progeny with high levels of P element transposition and
327 temperature-sensitive sterility. The reduced fertility of P-M F1 hybrids has been
328 attributed to lack of a piRNA response to specific transposable elements (Brennecke et
329 al., 2008), and we note that the sterility phenotype of P-M hybrids involves gonad
330 atrophy (Kelleher, 2016), which is reminiscent of the germ cell degeneration observed in
331 sterile late-generation *C. elegans* small RNA genome silencing mutants (Heestand et
332 al., 2018) (Fig 3). Defects in Piwi proteins lead to immediate sterility in *Drosophila*,
333 zebrafish and mouse, accompanied by transposon expression, transposition and by
334 increased levels of DNA damage, which implies that transposon-induced genome
335 instability could cause sterility of Piwi mutants (Juliano et al., 2011; Kelleher, 2016;
336 Siomi et al., 2011). However, analysis of effects of transposon copy number on P-M
337 hybrid dysgenesis indicated that transposon-induced genome instability only explains a
338 minor fraction of P-M hybrid sterility (Srivastav and Kelleher, 2017). Consistently, data
339 from our transgenerational model of sterility in response to heterochromatin
340 deterioration indicates that DNA damage is unlikely to be a central factor in small RNA
341 mutant sterility.

342 We addressed the mechanism that evokes sterility by discovering pronounced P
343 granule defects in sterile but not fertile late-generation animals (Updike and Strome,

344 2010). The common sterility phenotypes of *pgl-1* mutants, P granule RNAi treated
345 animals and small RNA genome silencing mutants imply that germ granule defects are
346 likely to cause sterility in response to heterochromatin dysfunction. Furthermore, our
347 data suggest that univalent chromosomes that are specifically observed in oocytes of
348 sterile small RNA genome silencing animals are a secondary consequence of P granule
349 dysfunction that indirectly disrupts a meiotic process (Hillers K.J. et al., 2017; Loidl,
350 2016). When RNA from sterile generation *nrde-1* and *nrde-4* mutant L4 larvae and from
351 late-generation *prg-1* mutants was examined, we failed to observe consistent depletion
352 of any gene whose knockdown is known to disrupt P granule formation (Updike and
353 Strome, 2010), suggesting that the mechanism by which P granules are disrupted in
354 *prg-1*, *nrde-1* and *nrde-4* mutants may be post-transcriptional. In addition, a lack of
355 commonly misregulated genes between sterile small RNA mutants and P granule
356 defective animals suggests that the reproductive arrest that occurs in response to P
357 granule dysfunction is orchestrated at a post-transcriptional level, at least at the L4
358 larval stage immediately prior to germ cell atrophy (Heestand et al., 2018). It is possible
359 that RNA or protein components of P granules are released at sterility to promote
360 reproductive arrest (Updike and Strome, 2010).

361 We found that some sterile *pgl-1* mutants could recover at permissive
362 temperature, resulting in growth of the germline and fertility (Fig. 3i-j), as previously
363 observed for sterile late-generations *prg-1* mutants whose germlines were in a
364 quiescent state of Adult Reproductive Diapause (Heestand et al., 2018). Given that *prg-*
365 *1* mutant germ cells may transmit a form of heritable stress that occurs in response to
366 heterochromatin dysfunction (Heestand et al., 2018), our results suggest that P granule

367 dysfunction could represent a general mechanism for orchestrating reproductive arrest
368 in the context of stress-induced Adult Reproductive Diapause. Possibly consistent with
369 our observations, sterile mouse mutants with defects in piRNA biogenesis have been
370 reported to display germ granule defects (Chuma et al., 2006; Zheng and Wang, 2012).
371 We suggest that germ granule dysfunction could explain the sterility observed in P-M
372 hybrid dysgenesis and the immediate sterility phenotype of Piwi mutants in several
373 species (Juliano et al., 2011; Kelleher, 2016; Siomi et al., 2011). Environmental stresses
374 such as starvation can also evoke reproductive arrest (Angelo and Van Gilst, 2009), and
375 it is possible that altered germ granule integrity could represent a response mechanism
376 to a variety of stresses. A more speculative consideration is that germ granule
377 dysfunction might contribute to the rise in human infertility and associated fertility
378 treatment in recent decades, which has been attributed to factors such as psychological
379 stress, caffeine consumption and pollutants (Homan et al., 2007; Younglai et al., 2005).
380 Small RNA silencing proteins such as CSR-1, PRG-1 or HRDE-1 are localized to
381 P granules, and it has been hypothesized that dysfunction of pro- and anti-silencing
382 small RNA pathways associated with P granules could be the cause of sterility in small
383 RNA genome silencing mutants (de Albuquerque et al., 2015; Phillips et al., 2015). Our
384 data is generally consistent with this hypothesis, as physical disruption of P granule
385 integrity is likely to generally perturb small RNA silencing pathways. However, we found
386 that few transposons were mis-regulated in P granule deficient L4 larvae, indicating that
387 the reproductive arrest phenotype that occurs in response of P granule disruption does
388 not cause pronounced desilencing of many heterochromatic segments of the genome.

389 Our results establish a novel framework for considering inheritance in the context
390 of epigenetic stress and how this can evoke transgenerational sterility. We suggest that
391 the sterility we describe in response to epigenome dysfunction represents a
392 developmental arrest mechanism to protect the genome or epigenome in times of
393 stress. We note that transposons and viruses are central targets of the small RNA
394 genome silencing system and are likely to be in a continuous arms race between
395 parasite and host, where components of P granules that protect the host are likely to be
396 targeted (Updike and Strome, 2010). It may therefore be reasonable to hypothesize the
397 evolution of a reproductive arrest mechanism in the context of an attack on the P
398 granule silencing system that is predicated on disrupting the integrity of P granules
399 themselves.
400

401 **Materials and Methods**
402
403 Strains
404 All strains were cultured at 20°C or 25°C on Nematode Growth Medium (NGM) plates
405 seeded with *E. coli* OP50. Strains used include Bristol N2 wild type, *hrde-1(tm1200) III,*
406 *rsd-6(yp11) I, nrde-1(yp4) III, nrde-2(gg95) II, nrde-4 (gg131) IV, prg-1 (n4357) I, prg-1*
407 *(tm872) I, mut-14 (pk730) V,* and *rbr-2(tm1231) IV.*
408

409 RNAi Assay
410 Feeding RNAi plates harboring host bacteria HT115(DE3) engineered to express "quad"
411 dsRNA (targeting P granules) were obtained from Susan Strome (Knutson et al., 2017;
412 Updike et al., 2014). L1 larvae were placed onto freshly prepared feeding RNAi plates

413 with dsRNA induced by 1 mM IPTG (isopropyl-β-D(-)-thiogalactopyranoside) and were
414 transferred after 1 generation at 25°C and collected at F2 adults as described in
415 Knutson et al., 2017 for DAPI staining, oocyte and germline analysis.
416
417 DAPI staining and Scoring
418 DAPI staining was performed as previously described (Ahmed and Hodgkin, 2000).
419 Briefly, L4 larvae were selected from sibling plates and sterile adults were singled as
420 late L4s, observed 24 hours later for confirmed sterility, and then stained 48 hours after
421 collection. Univalents were scored by counting DAPI bodies in the -1 to -4 oocytes.
422 Germline profiles were scored using the method outlined in Heestand et al 2018
423 (Heestand et al., 2018).
424
425 Statistical Analysis
426 Statistical analysis was performed as previously described (Heestand et al., 2018).
427 Briefly, statistical analysis was performed using the R statistical environment (R Core
428 Team, 2013). For germline phenotypes, contingency tables were constructed and
429 pairwise Chi Square tests with Bonferroni correction was used to determine significant
430 differences in in germline phenotype distributions. The significance of the DNA damage
431 response analysis was determined by a Kruskal-Wallis test, followed by a Mann-
432 Whitney test between individual samples. P-values were adjusted with Bonferroni
433 correction when multiple comparisons were performed.
434
435 RNA extraction and sequencing

436 Animals were grown at 20°C on 60 mm NGM plates seeded with OP50 bacteria. RNA
437 was extracted using Trizol (Ambion) followed by isopropanol precipitation. Library
438 preparation and sequencing was performed at the UNC School of Medicine High-
439 Throughput Sequencing Facility (HTSF). Libraries were were prepared from ribosome-
440 depleted RNA and sequenced on an Illumina Hiseq 2500.
441
442 RNA-seq Analysis
443 The following publicly available RNA-seq datasets were download from the Gene
444 Expression Omnibus (https://www.ncbi.nlm.nih.gov/geo/): GSE92690 (P granule RNAi
445 experiment) and GSE87524 (*prg-1* experiment). Adapter trimming was performed as
446 required using the bbduk.sh script from the BBmap suite (Bushnell, n.d.) and custom
447 scripts. Reads were then mapped to the *C. elegans* genome (WS251) using hisat2 (Kim
448 et al., 2013) with default settings and read counts were assigned to protein-coding
449 genes using the featureCounts utility from the Subread package (Liao et al., 2014) . For
450 multimapping reads, each mapping locus was assigned a count of 1/n where n=number
451 of hits. Differentially expressed genes were identified using DESeq2, and were defined
452 as changing at least 2-fold with FDR-corrected p-value < 0.01. For analysis of
453 transposon RNAs, reads were mapped to the C. elegans transposon consensus
454 sequences downloaded from Repbase (http://www.girinst.org/repbase/) with bowtie
455 (Langmead et al., 2009) using the options -M 1 -v 2. Transposons with fewer than 10
456 counts in each sample were excluded from further analysis. Counts were normalized to
457 the total number of mapped reads for each library for the prg-1 dataset, or to the total
458 number of non-ribosomal mapped reads for all other datasets. A pseudocount of 1 was

459 added to each value to avoid division by zero errors. Analysis of sequencing data and
460 plot creation was performed using the R statistical computing environment (R Core
461 Team, 2013).
462
463 Accession numbers: RNA-seq data reported in this study have been submitted to the
464 GEO database and will be available at the time of publication.
465
466 Immunofluorescence
467 Adult hermaphrodites raised at 20°C or 25°C were dissected in M9 buffer and flash
468 frozen on dry ice before fixation for 1 min in methanol at -20°C. After washing in PBS
469 supplemented with 0.1% Tween-20 (PBST), primary antibody diluted in in PBST was
470 used to immunostain overnight at 4 °C in a humid chamber. Primaries used were 1:50
471 OIC1D4 (Developmental Studies Hybridoma Bank). Secondary antibody staining was
472 performed by using a Cy3 donkey anti-mouse or Cy-5 donkey anti-rabbit overnight at
473 4°C. All images were obtained using a LSM 710 laser scanning confocal and were
474 taken using same settings as control samples. Images processed using ImageJ.
475
476 DNA Damage Assay
477 Worms that were close to sterility were isolated and defined as sterile if they did not
478 have any offspring as day 3 adults at 20˚C or day 2 adults at 25˚C. Fertile siblings of
479 sterile worms were defined as 'close to sterility'. The presence of the DNA damage
480 response was determined by using a phospho-specific antibody targeting the
481 phosphorylated consensus target site of ATM and ATR kinases (pS/TQ) (Cell Signaling

482 Technology). This antibody has only been shown to stain a DNA damage response in
483 the germline and was used as previously described (Vermezovic et al., 2012).
484
485 **Acknowledgments:** We thank members of the Ahmed lab for critical reading of the
486 manuscript and Jacinth Mitchell for wildtype control, *nrde-1* and *nrde-2* RNA-seq data.
487 Some strains were provided by the CGC, which is funded by NIH Office of Research
488 Infrastructure Programs (P40 OD010440). This study was supported by NIH grants F32
489 GM120809 (K.B) and RO1 GM083048 (S.A). M.S. was supported by a DFG postdoc
490 fellowship.
491
492 **Competing interests:** Authors declare no competing interests.
493
494 **Author contributions:** K.B., B.H., M.S. and S.F. performed experiments. S.F. analyzed
495 the data. K.B., B.H., M.S., S.F. and S.A. wrote manuscript.
496
497 **References:**

498 Ahmed, S., Hodgkin, J., 2000. MRT-2 checkpoint protein is required for germline
499 immortality and telomere replication in C. elegans. Nature 403, 159–64.
500 https://doi.org/10.1038/35003120

501 Alvares, S.M., Mayberry, G.A., Joyner, E.Y., Lakowski, B., Ahmed, S., 2014. H3K4
502 demethylase activities repress proliferative and postmitotic aging. Aging Cell 13,
503 245–253. https://doi.org/10.1111/acel.12166

504 Angelo, G., Van Gilst, M.R., 2009. Starvation Protects Germline Stem Cells and
505 Extends Reproductive Longevity in C. elegans. Science (80-.). 326, 954–958.
506 https://doi.org/10.1126/science.1178343

507 Aravin, A.A., Hannon, G.J., Brennecke, J., 2007. The Piwi-piRNA pathway provides an
508 adaptive defense in the transposon arms race. Science 318, 761–4.
509 https://doi.org/10.1126/science.1146484

510 Ashe, A., Sapetschnig, A., Weick, E.-M., Mitchell, J., Bagijn, M.P., Cording, A.C.,
511 Doebley, A.-L., Goldstein, L.D., Lehrbach, N.J., Le Pen, J., Pintacuda, G.,
512 Sakaguchi, A., Sarkies, P., Ahmed, S., Miska, E.A., 2012. piRNAs can trigger a
513 multigenerational epigenetic memory in the germline of C. elegans. Cell 150, 88–
514 99. https://doi.org/10.1016/j.cell.2012.06.018

515 Batista, P.J., Ruby, J.G., Claycomb, J.M., Chiang, R., Fahlgren, N., Kasschau, K.D.,
516 Chaves, D.A., Gu, W., Vasale, J.J., Duan, S., Conte, D., Luo, S., Schroth, G.P.,
517 Carrington, J.C., Bartel, D.P., Mello, C.C., 2008. PRG-1 and 21U-RNAs interact to
518 form the piRNA complex required for fertility in C. elegans. Mol. Cell 31, 67–78.
519 https://doi.org/10.1016/j.molcel.2008.06.002

520 Brennecke, J., Malone, C.D., Aravin, A.A., Sachidanandam, R., Stark, A., Hannon, G.J.,
521 2008. An epigenetic role for maternally inherited piRNAs in transposon silencing.
522 Science 322, 1387–92. https://doi.org/10.1126/science.1165171

523 Buckley, B.A., Burkhart, K.B., Gu, S.G., Spracklin, G., Kershner, A., Fritz, H., Kimble, J.,
524 Fire, A., Kennedy, S., 2012. A nuclear Argonaute promotes multigenerational
525 epigenetic inheritance and germline immortality. Nature 489, 447–451.

526 https://doi.org/10.1038/nature11352

527 Burkhart, K.B., Guang, S., Buckley, B.A., Wong, L., Bochner, A.F., Kennedy, S., 2011.
528 A pre-mRNA-associating factor links endogenous siRNAs to chromatin regulation.
529 PLoS Genet. 7, e1002249. https://doi.org/10.1371/journal.pgen.1002249

530 Bushnell, B., n.d. BBMap short-read aligner [WWW Document]. URL
531 https://sourceforge.net/projects/bbmap/ (accessed 4.22.18).

532 Chuma, S., Hosokawa, M., Kitamura, K., Kasai, S., Fujioka, M., Hiyoshi, M., Takamune,
533 K., Noce, T., Nakatsuji, N., 2006. Tdrd1/Mtr-1, a tudor-related gene, is essential for
534 male germ-cell differentiation and nuage/germinal granule formation in mice. Proc.
535 Natl. Acad. Sci. 103, 15894–15899. https://doi.org/10.1073/pnas.0601878103

536 Das, P.P., Bagijn, M.P., Goldstein, L.D., Woolford, J.R., Lehrbach, N.J., Sapetschnig,
537 A., Buhecha, H.R., Gilchrist, M.J., Howe, K.L., Stark, R., Matthews, N., Berezikov,
538 E., Ketting, R.F., Tavar?, S., Miska, E.A., 2008. Piwi and piRNAs Act Upstream of
539 an Endogenous siRNA Pathway to Suppress Tc3 Transposon Mobility in the
540 Caenorhabditis elegans Germline. Mol. Cell 31, 79–90.
541 https://doi.org/10.1016/j.molcel.2008.06.003

542 de Albuquerque, B.F.M., Placentino, M., Ketting, R.F., 2015. Maternal piRNAs Are
543 Essential for Germline Development following De Novo Establishment of Endo-
544 siRNAs in Caenorhabditis elegans. Dev. Cell 34, 448–56.
545 https://doi.org/10.1016/j.devcel.2015.07.010

546 Guang, S., Bochner, A.F., Burkhart, K.B., Burton, N., Pavelec, D.M., Kennedy, S., 2010.
547 Small regulatory RNAs inhibit RNA polymerase II during the elongation phase of

548 transcription. Nature 465, 1097–1101. https://doi.org/10.1038/nature09095

549 Guang, S., Bochner, A.F., Pavelec, D.M., Burkhart, K.B., Harding, S., Lachowiec, J.,
550 Kennedy, S., 2008. An Argonaute Transports siRNAs from the Cytoplasm to the
551 Nucleus. Science (80-.). 321, 537–541. https://doi.org/10.1126/science.1157647

552 Heestand, B., Simon, M., Frenk, S., Titov, D., Ahmed, S., 2018. Transgenerational
553 Sterility of Piwi Mutants Represents a Dynamic Form of Adult Reproductive
554 Diapause. Cell Rep. 23, 156–171. https://doi.org/10.1016/j.celrep.2018.03.015

555 Hillers K.J., Jantsch V., Martinez-Perez E., Yanowitz J.L, 2017. Meiosis.
556 https://doi.org/10.1895/wormbook.1.178.1

557 Homan, G.F., Davies, M., Norman, R., 2007. The impact of lifestyle factors on
558 reproductive performance in the general population and those undergoing infertility
559 treatment: a review. Hum. Reprod. Update 13, 209–223.
560 https://doi.org/10.1093/humupd/dml056

561 Juliano, C., Wang, J., Lin, H., 2011. Uniting Germline and Stem Cells: The Function of
562 Piwi Proteins and the piRNA Pathway in Diverse Organisms. Annu. Rev. Genet. 45,
563 447–469. https://doi.org/10.1146/annurev-genet-110410-132541

564 Käser-Pébernard, S., Müller, F., Wicky, C., 2014. LET-418/Mi2 and SPR-5/LSD1
565 cooperatively prevent somatic reprogramming of C. elegans germline stem cells.
566 Stem cell reports 2, 547–59. https://doi.org/10.1016/j.stemcr.2014.02.007

567 Katz, D.J., Edwards, T.M., Reinke, V., Kelly, W.G., 2009. A C. elegans LSD1
568 demethylase contributes to germline immortality by reprogramming epigenetic
569 memory. Cell 137, 308–20. https://doi.org/10.1016/j.cell.2009.02.015

570 Kawasaki, I., Shim, Y.H., Kirchner, J., Kaminker, J., Wood, W.B., Strome, S., 1998.
571 PGL-1, a predicted RNA-binding component of germ granules, is essential for
572 fertility in C. elegans. Cell 94, 635–45.

573 Kelleher, E.S., 2016. Reexamining the P-Element Invasion of Drosophila melanogaster
574 Through the Lens of piRNA Silencing. Genetics 203, 1513–1531.
575 https://doi.org/10.1534/genetics.115.184119

576 Ketting, R.F., Haverkamp, T.H., van Luenen, H.G., Plasterk, R.H., 1999. Mut-7 of C.
577 elegans, required for transposon silencing and RNA interference, is a homolog of
578 Werner syndrome helicase and RNaseD. Cell 99, 133–41.

579 Kidwell, M.G., Kidwell, J.F., Sved, J.A., 1977. Hybrid Dysgenesis in DROSOPHILA
580 MELANOGASTER: A Syndrome of Aberrant Traits Including Mutation, Sterility and
581 Male Recombination. Genetics 86, 813–33.

582 Kim, D., Pertea, G., Trapnell, C., Pimentel, H., Kelley, R., Salzberg, S.L., 2013.
583 TopHat2: accurate alignment of transcriptomes in the presence of insertions,
584 deletions and gene fusions. Genome Biol. 14, R36. https://doi.org/10.1186/gb-
585 2013-14-4-r36

586 Kim, S.T., Lim, D.S., Canman, C.E., Kastan, M.B., 1999. Substrate specificities and
587 identification of putative substrates of ATM kinase family members. J. Biol. Chem.
588 274, 37538–43.

589 Knutson, A.K.K., Egelhofer, T., Rechtsteiner, A., Strome, S., 2017. Germ Granules
590 Prevent Accumulation of Somatic Transcripts in the Adult Caenorhabditis elegans
591 Germline. Genetics 206.

592 Langmead, B., Trapnell, C., Pop, M., Salzberg, S.L., 2009. Ultrafast and memory-
593 efficient alignment of short DNA sequences to the human genome. Genome Biol.
594 10, R25. https://doi.org/10.1186/gb-2009-10-3-r25

595 Liao, Y., Smyth, G.K., Shi, W., 2014. featureCounts: an efficient general purpose
596 program for assigning sequence reads to genomic features. Bioinformatics 30,
597 923–930. https://doi.org/10.1093/bioinformatics/btt656

598 Loidl, J., 2016. Conservation and Variability of Meiosis Across the Eukaryotes. Annu.
599 Rev. Genet. 50, 293–316. https://doi.org/10.1146/annurev-genet-120215-035100

600 Luteijn, M.J., Ketting, R.F., 2013. PIWI-interacting RNAs: from generation to
601 transgenerational epigenetics. Nat. Rev. Genet. 14, 523–534.
602 https://doi.org/10.1038/nrg3495

603 McMurchy, A.N., Stempor, P., Gaarenstroom, T., Wysolmerski, B., Dong, Y.,
604 Aussianikava, D., Appert, A., Huang, N., Kolasinska-Zwierz, P., Sapetschnig, A.,
605 Miska, E.A., Ahringer, J., 2017. A team of heterochromatin factors collaborates with
606 small RNA pathways to combat repetitive elements and germline stress. Elife 6.
607 https://doi.org/10.7554/eLife.21666

608 Min, H., Shim, Y.-H., Kawasaki, I., 2016. Loss of PGL-1 and PGL-3, members of a
609 family of constitutive germ-granule components, promotes germline apoptosis in C.
610 elegans. J. Cell Sci. 129, 341–353. https://doi.org/10.1242/jcs.174201

611 Ni, J.Z., Kalinava, N., Chen, E., Huang, A., Trinh, T., Gu, S.G., 2016. A
612 transgenerational role of the germline nuclear RNAi pathway in repressing heat
613 stress-induced transcriptional activation in C. elegans. Epigenetics Chromatin 9, 3.

614 https://doi.org/10.1186/s13072-016-0052-x

615 Padilla, P.A., Ladage, M.L., 2012. Suspended animation, diapause and quiescence.
616 Cell Cycle 11, 1672–1679. https://doi.org/10.4161/cc.19444

617 Phillips, C.M., Brown, K.C., Montgomery, B.E., Ruvkun, G., Montgomery, T.A., 2015.
618 piRNAs and piRNA-Dependent siRNAs Protect Conserved and Essential
619 C. elegans Genes from Misrouting into the RNAi Pathway. Dev. Cell 34, 457–465.
620 https://doi.org/10.1016/j.devcel.2015.07.009

621 Phillips, C.M., Montgomery, T.A., Breen, P.C., Ruvkun, G., 2012. MUT-16 promotes
622 formation of perinuclear mutator foci required for RNA silencing in the C. elegans
623 germline. Genes Dev. 26, 1433–44. https://doi.org/10.1101/gad.193904.112

624 R Core Team, 2013. R: A language and environment for statistical computing. R
625 Found. Stat. Comput.

626 Robert, V.J., Mercier, M.G., Bedet, C., Janczarski, S., Merlet, J., Garvis, S., Ciosk, R.,
627 Palladino, F., 2014. The SET-2/SET1 Histone H3K4 Methyltransferase Maintains
628 Pluripotency in the Caenorhabditis elegans Germline, Cell Reports.
629 https://doi.org/10.1016/j.celrep.2014.09.018

630 Sakaguchi, A., Sarkies, P., Simon, M., Doebley, A.-L., Goldstein, L.D., Hedges, A.,
631 Ikegami, K., Alvares, S.M., Yang, L., LaRocque, J.R., Hall, J., Miska, E.A., Ahmed,
632 S., 2014. Caenorhabditis elegans RSD-2 and RSD-6 promote germ cell immortality
633 by maintaining small interfering RNA populations. Proc. Natl. Acad. Sci. U. S. A.
634 111, E4323-31. https://doi.org/10.1073/pnas.1406131111

635 Simon, M., Sarkies, P., Ikegami, K., Doebley, A.-L., Goldstein, L.D., Mitchell, J.,

636 Sakaguchi, A., Miska, E.A., Ahmed, S., 2014. Reduced insulin/IGF-1 signaling
637 restores germ cell immortality to Caenorhabditis elegans Piwi mutants. Cell Rep. 7,
638 762–73. https://doi.org/10.1016/j.celrep.2014.03.056

639 Siomi, M.C., Sato, K., Pezic, D., Aravin, A.A., 2011. PIWI-interacting small RNAs: the
640 vanguard of genome defence. Nat. Rev. Mol. Cell Biol. 12, 246–258.
641 https://doi.org/10.1038/nrm3089

642 Smelick, C., Ahmed, S., 2005. Achieving immortality in the C. elegans germline. Ageing
643 Res. Rev. 4, 67–82. https://doi.org/10.1016/j.arr.2004.09.002

644 Spracklin, G., Fields, B., Wan, G., Vijayendran, D., Wallig, A., Shukla, A., Kennedy, S.,
645 2017. Identification and Characterization of Caenorhabditis elegans RNAi
646 Inheritance Machinery. Genetics.

647 Srivastav, S.P., Kelleher, E.S., 2017. Paternal Induction of Hybrid Dysgenesis in
648 *Drosophila melanogaster* Is Weakly Correlated with Both *P* -Element and *hobo*
649 Element Dosage. G3: Genes|Genomes|Genetics 7, 1487–1497.
650 https://doi.org/10.1534/g3.117.040634

651 Strome, S., Wood, W.B., 1982. Immunofluorescence visualization of germ-line-specific
652 cytoplasmic granules in embryos, larvae, and adults of Caenorhabditis elegans.
653 Proc. Natl. Acad. Sci. U. S. A. 79, 1558–62.

654 Sung, M., Kawasaki, I., Shim, Y.-H., 2017. Depletion of *cdc-25.3* , a
655 *Caenorhabditis elegans* orthologue of *cdc25* , increases physiological germline
656 apoptosis. FEBS Lett. 591, 2131–2146. https://doi.org/10.1002/1873-3468.12717

657 Tatar, M., Yin, C., 2001. Slow aging during insect reproductive diapause: why

658 butterflies, grasshoppers and flies are like worms. Exp. Gerontol. 36, 723–38.

659 Updike, D., Strome, S., 2010. P Granule Assembly and Function in Caenorhabditis
660 elegans Germ Cells. J. Androl. 31, 53–60.
661 https://doi.org/10.2164/jandrol.109.008292

662 Updike, D.L., Hachey, S.J., Kreher, J., Strome, S., 2011. P granules extend the nuclear
663 pore complex environment in the *C. elegans* germ line. J. Cell Biol. 192, 939–948.
664 https://doi.org/10.1083/jcb.201010104

665 Updike, D.L., Knutson, A.K., Egelhofer, T.A., Campbell, A.C., Strome, S., 2014. Germ-
666 Granule Components Prevent Somatic Development in the C. elegans Germline.
667 Curr. Biol. 24, 970–975. https://doi.org/10.1016/j.cub.2014.03.015

668 Vermezovic, J., Stergiou, L., Hengartner, M.O., d'Adda di Fagagna, F., 2012.
669 Differential regulation of DNA damage response activation between somatic and
670 germline cells in Caenorhabditis elegans. Cell Death Differ. 19, 1847–1855.
671 https://doi.org/10.1038/cdd.2012.69

672 Younglai, E. V., Holloway, A.C., Foster, W.G., 2005. Environmental and occupational
673 factors affecting fertility and IVF success. Hum. Reprod. Update 11, 43–57.
674 https://doi.org/10.1093/humupd/dmh055

675 Zeller, P., Padeken, J., van Schendel, R., Kalck, V., Tijsterman, M., Gasser, S.M., 2016.
676 Histone H3K9 methylation is dispensable for Caenorhabditis elegans development
677 but suppresses RNA:DNA hybrid-associated repeat instability. Nat. Genet. 48,
678 1385–1395. https://doi.org/10.1038/ng.3672

679 Zheng, K., Wang, P.J., 2012. Blockade of Pachytene piRNA Biogenesis Reveals a

680 Novel Requirement for Maintaining Post-Meiotic Germline Genome Integrity. PLoS
681 Genet. 8, e1003038. https://doi.org/10.1371/journal.pgen.1003038
682
683
684
685
686
687
688
689
690
691
692

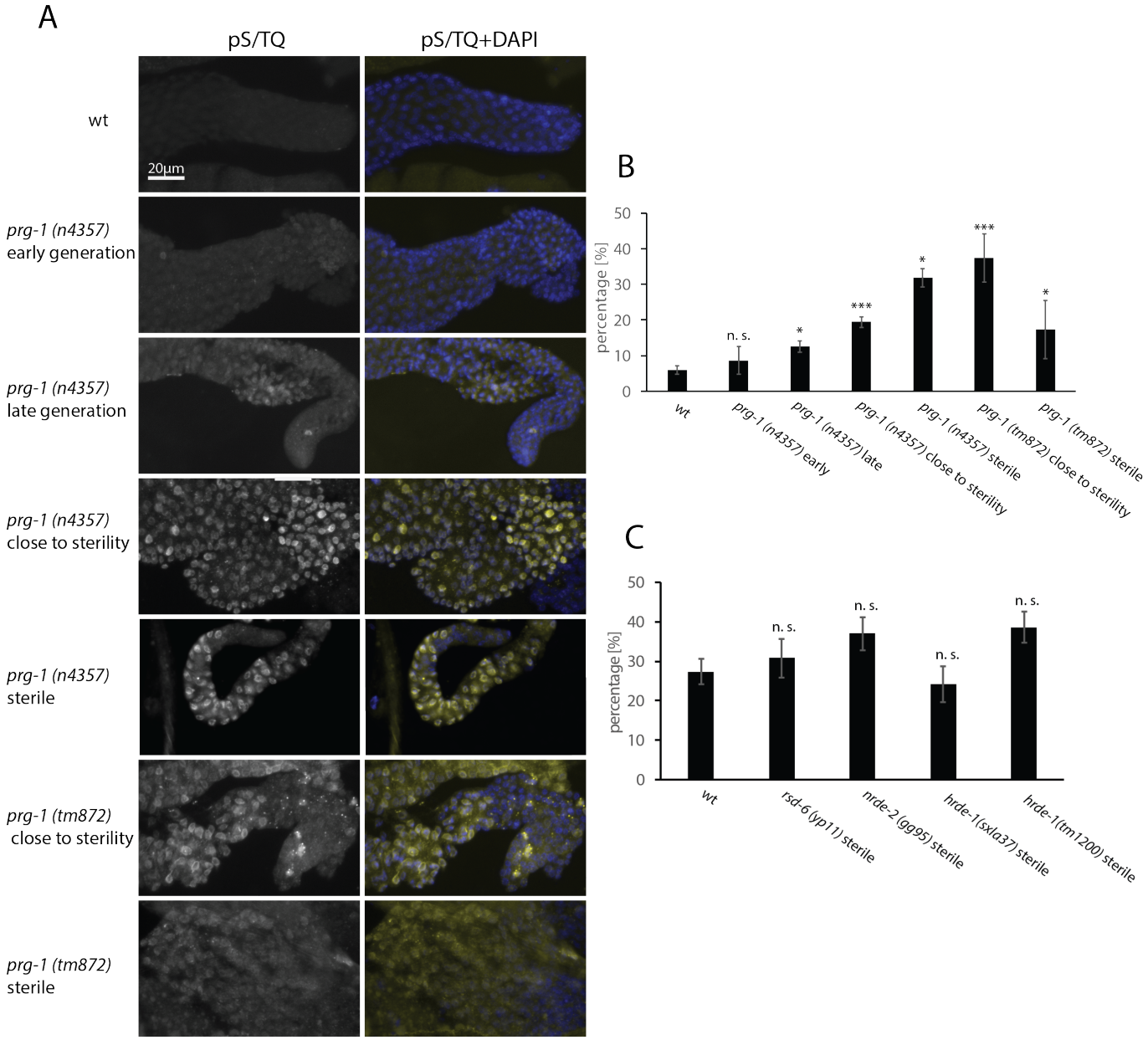

693

694 **Figure 1: DNA Damage Response is variable in small RNA genome silencing**

695 **mutants prior to and at sterility. (A)** Staining of pS/TQ in wildtype, *prg-1(n4357) and*

696 *prg-1(tm876)* mutants. pS/TQ(grey and yellow) and DAPI(blue) **(B)** Quantification of

697 pS/TQ staining in 20°C wildtype and *prg-1* mutants at different levels of fertility. **(C)**

698 Quantification of pS/TQ staining in 25°C wildtype and small RNA genomic silencing

699 mutants at sterility. P-values were obtained by comparing sample groups in a Mann-

700 Whitney U test (p-value: P > 0.05 = n. s., P < 0.05 = *, P = <0.01 = **, P =< 0.001 = ***

701 compared to wildtype)

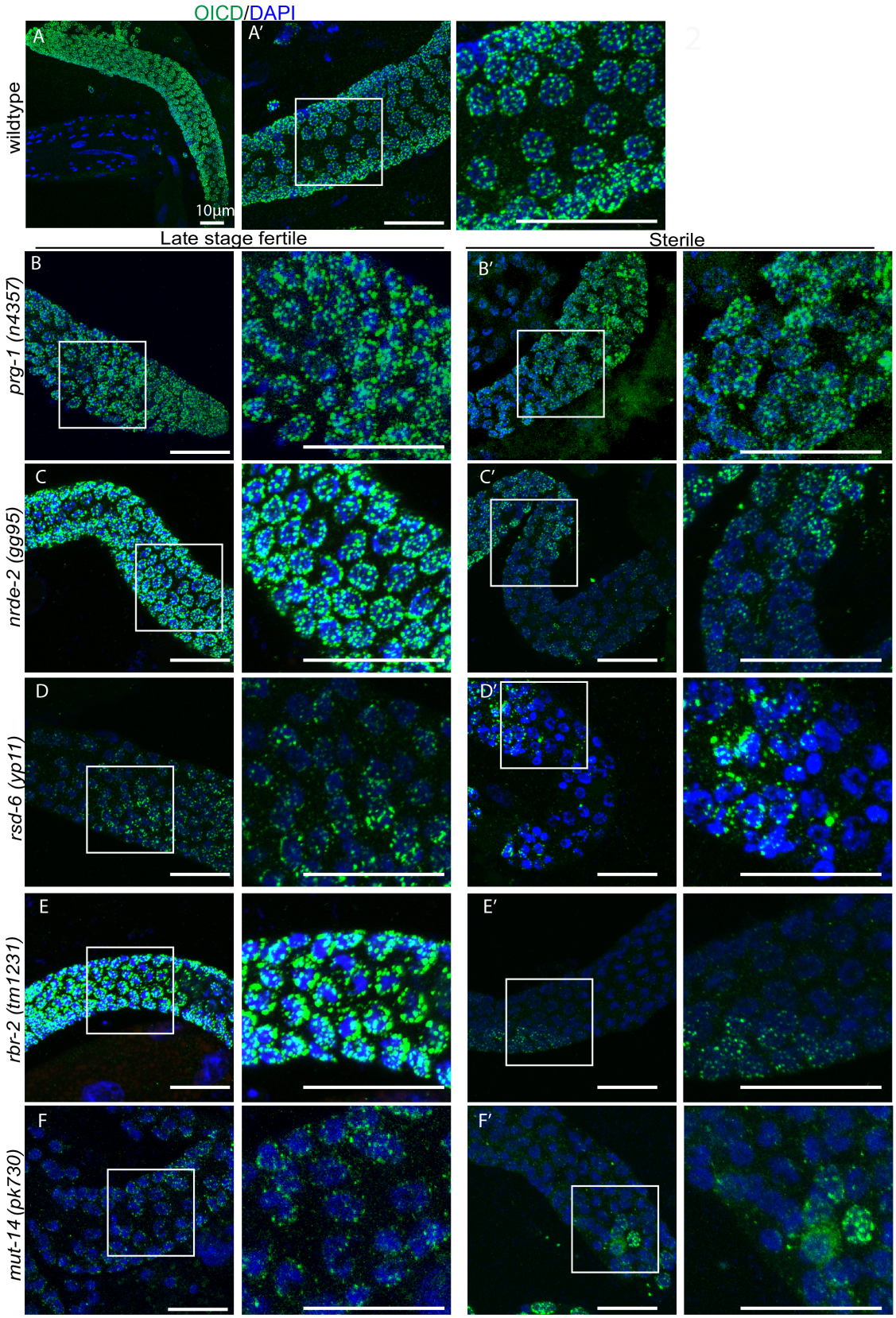
OICD/DAPI
A
A′
wildtype
10µm
Late stage fertile
Sterile
B
B′
prg-1 (n4357)
C
C′
nrde-2 (gg95)
D
D′
rsd-6 (yp11)
E
E′
rbr-2 (tm1231)
F
F′
mut-14 (pk730)

702

703 **Figure 2: At sterility, partial loss of P granule staining occurred in *prg-1* and**
704 **temperature-sensitive mutants.** Germlines of sterile Day 2-3 adult animals were
705 stained using the OIC1D4 antibody against P granules (green) and DAPI (blue). **(A-A')**
706 Control animals contain uniform puncta of P granule staining surrounding each nuclei.
707 **(B-F)** Late generation fertile *prg-1, rsd-6*, *nrde-2*, *rbr-2*, and *mut-14* animals displayed
708 relatively normal P granule staining in the germlines. **(B'-F')** *prg-1*, *nrde-2*, *rsd-6, rbr-2,*
709 and *mut-14* sterile animals all exhibited some degree of germ cell P granule loss.
710

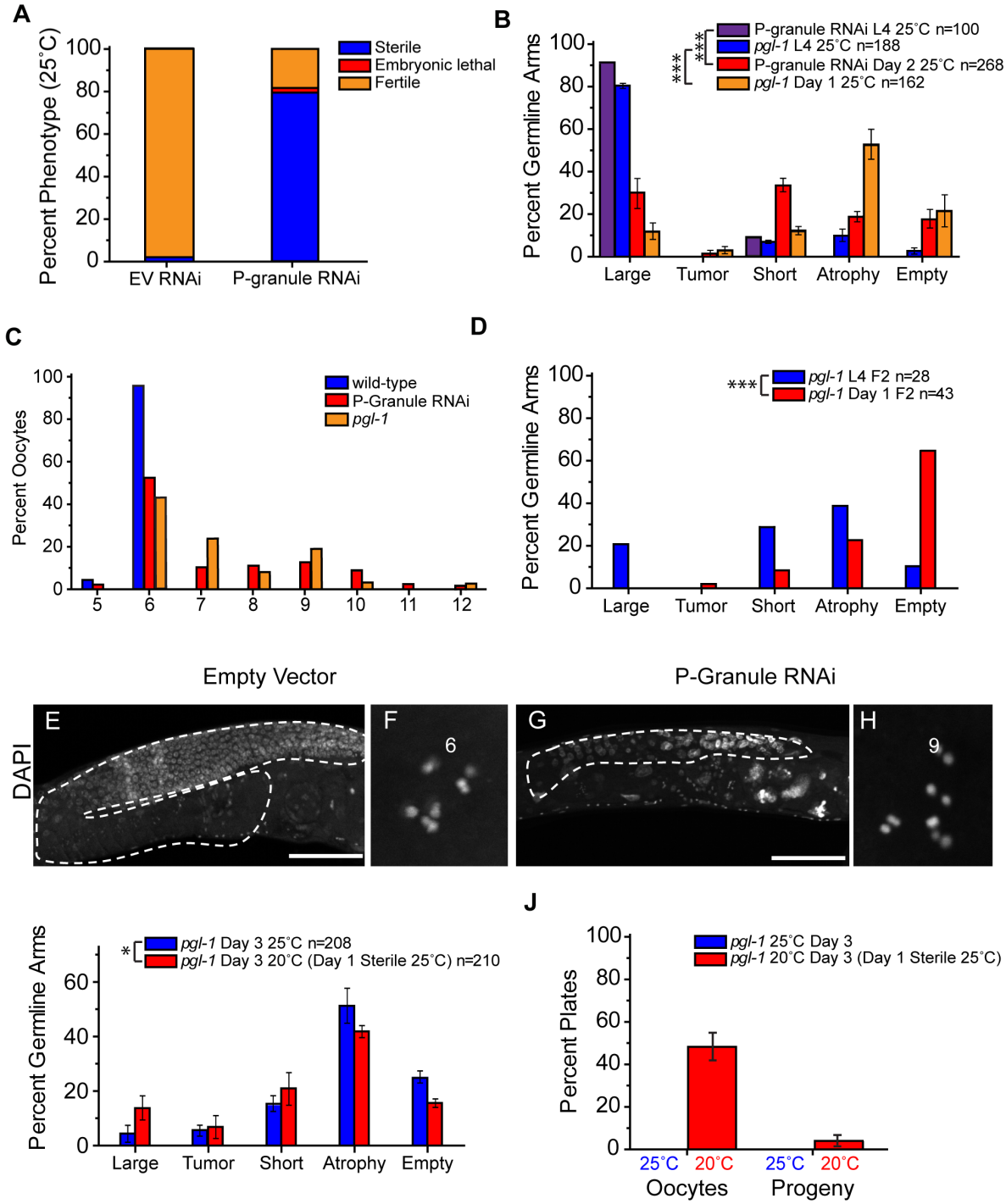

Figure 3: Disruption of P granules by RNAi or loss of *pgl-1* resulted in similar phenotypes. (A) F2 wild-type (N2) worms on Empty Vector (EV) or P granule RNAi at 25°C were scored for sterility, embryonic lethality, or fertility. n=16-30 worms per

715 condition, 2 independent experiments. **(B)** F1 L4 *pgl-1* mutants and F2 L4 P granule
716 RNAi treated animals stained by DAPI contained mostly large germlines while adults
717 exhibited a range of germline phenotypes from empty to large. **(C)** F1 *pgl-1* mutants and
718 F2 P granule RNAi treated animals contained oocytes with increased numbers of
719 univalents at sterility as measured by DAPI bodies n=151 wild-type, 81 P granule RNAi,
720 37 *pgl-1*. (D) Stained DAPI germlines of sterile F2 L4 and Day 1 *pgl-1* mutants. **(E-H)**
721 Representative DAPI images of germline and oocyte defects in empty vector treated
722 animals **(E,F)** and P granule RNAi treated animals **(G,H)** scale bar=10μm. **(I)** *pgl-1* F1
723 worms at 25°C were either DAPI stained as Day 3 adults (blue) or shifted to 20°C at
724 Day 1 and DAPI stained at Day 3 (red). **(I)** No sterile day 1 *pgl-1* F1 at 25°C laid
725 oocytes or progeny (n=35 plates, 350 worms). Sterile day 1 *pgl-1* shifted to 20°C (n=50
726 plates, 500 worms) gave rise to plates with oocytes and rarely progeny. Plates with
727 oocytes contained both oocytes and dead embryos. Plates with progeny contained
728 embryos that hatched to L1. For B,D,I *** $p<0.0001$, * $p=0.007$ Fisher's Chi Square test
729 with Bonferroni correction, n=total germlines scored, error bars are S.E.M.
730

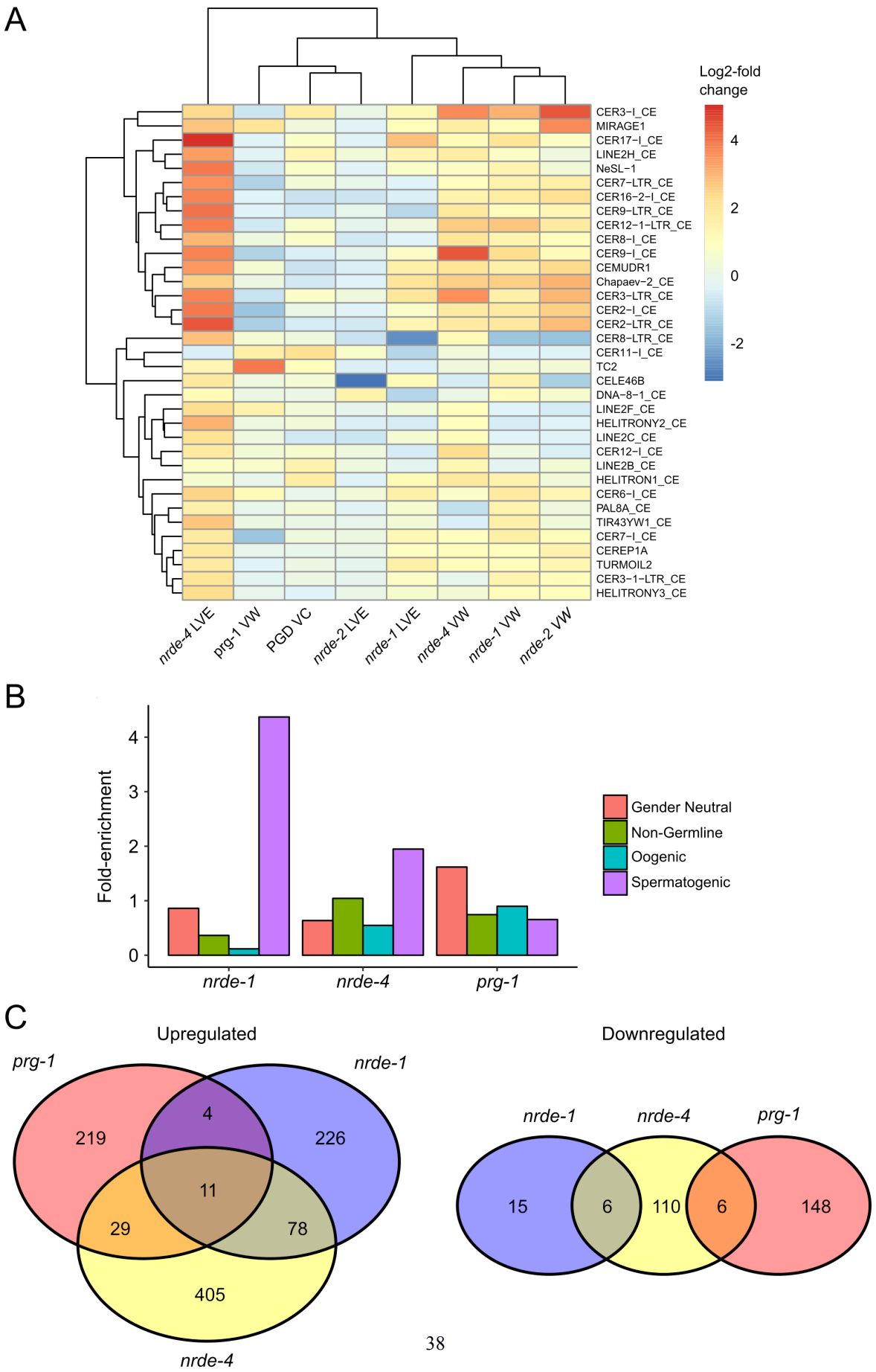
A
Log2-fold change
4
2
0
-2
CER3−I_CE
MIRAGE1
CER17−I_CE
LINE2H_CE
NeSL−1
CER7−LTR_CE
CER16−2−I_CE
CER9−LTR_CE
CER12−1−LTR_CE
CER8−I_CE
CER9−I_CE
CEMUDR1
Chapaev−2_CE
CER3−LTR_CE
CER2−I_CE
CER2−LTR_CE
CER8−LTR_CE
CER11−I_CE
TC2
CELE46B
DNA−8−1_CE
LINE2F_CE
HELITRONY2_CE
LINE2C_CE
CER12−I_CE
LINE2B_CE
HELITRON1_CE
CER6−I_CE
PAL8A_CE
TIR43YW1_CE
CER7−I_CE
CEREP1A
TURMOIL2
CER3−1−LTR_CE
HELITRONY3_CE
nrde-4 LVE
prg-1 VW
PGD VC
nrde-2 LVE
nrde-1 LVE
nrde-4 VW
nrde-1 VW
nrde-2 VW
B
Fold-enrichment
0
1
2
3
4
nrde-1
nrde-4
prg-1
Gender Neutral
Non-Germline
Oogenic
Spermatogenic
C
Upregulated
prg-1
nrde-1
nrde-4
219
4
226
11
29
78
405
Downregulated
nrde-1
nrde-4
prg-1
15
6
110
6
148

731

732 **Figure 4: Transcriptome profiling of germ granule deficient larvae and small RNA**
733 **genome silencing mutants. (A)** Log2-fold changes in transposon transcript abundance
734 in mutant vs wild-type (VW), late vs early generation (LVE) or P granule RNAi-treated vs
735 control (PGD VC). Transposons upregulated at least two-fold in *nrde-1*, *nrde-4* or *prg-*
736 *1(n4357)* are shown. **(B)** Enrichment of germline-expressed genes in genes upregulated
737 in small RNA mutants. **(C)** Number of genes up and downregulated in small RNA
738 mutants.

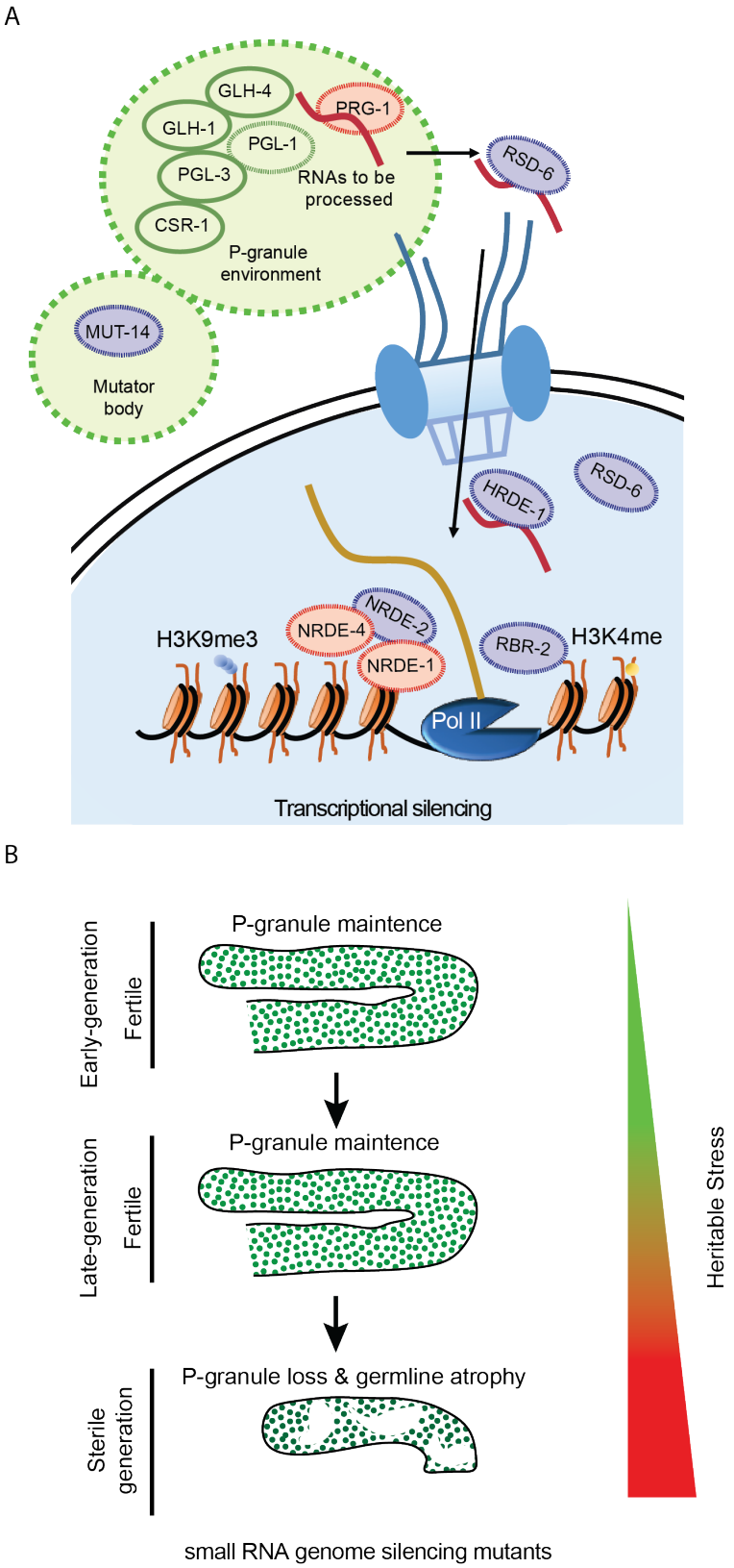

Figure 5: Model for P granule dysfunction in small RNA genome silencing

741 **mutants.** (**A**) Model of P granules and associated small RNA genome silencing
742 proteins. Green circles contain P granule components. Mutants in this paper that are
743 temperature-sensitive for germ cell immortality have blue outlines. Non-conditional
744 mutants have red outlines. **(B)** Model for accumulating Heritable Stress in small RNA
745 genome silencing mutants, which ultimately compromises P granule integrity.

746

747

748

749

750 **Table 1**

Genotype	<20% loss	>20%loss	p-value
wt	32	0	
prg-1 (tm872)	1	7	<.0001
prg-1 (n4357)	3	1	=.11
hrde-1 (tm1200)	0	31	<.0001
rsd-6 (yp11)	0	32	<.0001
nrde-2(gg95)	0	25	<.0001
rbr-2 (tm1231)	0	32	<.0001
nrde-4 (gg131)	17	5	=.008
mut-14 (pk730)	1	6	<.0001
nrde-1 (yp4)	4	6	<.0001

751

752 **Table 1: Quantification of P granule defects in the germline.**

753 Sterile small RNA genome silencing mutants were stained with P granule antibody.
754 Germlines arms were semi-qualitatively scored for P granules. If at least 20% of the arm
755 was missing P granules if was scored as loss and if 80% or more of the arm contained
756 P granules on DAPI-stained nuclei it was considered normal. Statistics were performed
757 using Fishers exact test.
758
759
760
761

762 **Supplemental Information**

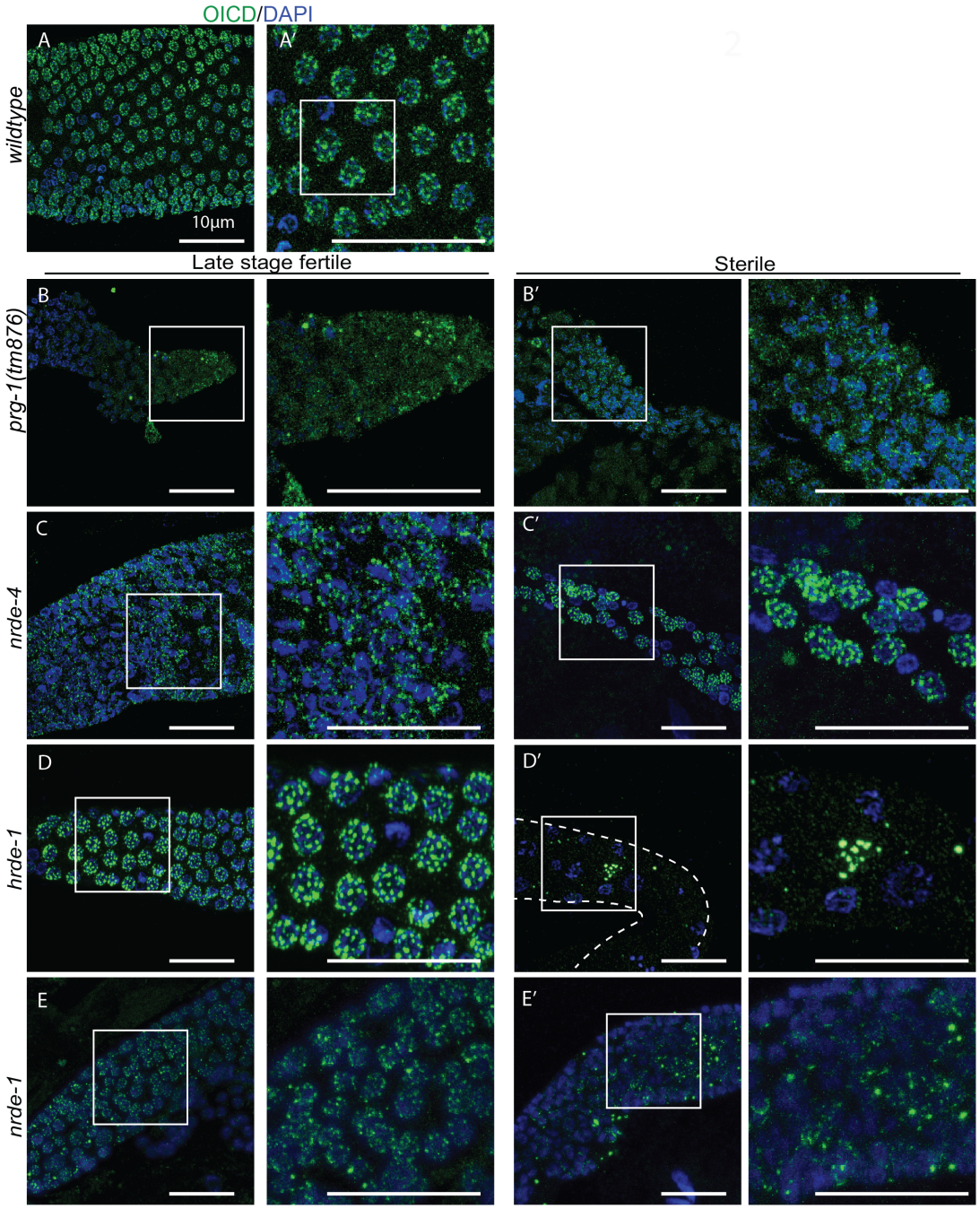

763

764 **Fig. S1. Related to Figure 2. P granule defects in *prg-1, nrde- 4, hrde-1 and nrde-1*.**
765 Germlines of sterile Day 2-3 adult animals were stained using the OIC1D4 antibody against P
766 granules (green) and DAPI (blue). (A-A') Control animals contain uniform puncta of P granule
767 staining surrounding each nuclei. (B-E) Late generation fertile *prg-1, nrde-4, hrde-1*, and *nrde-1*

768 animals displayed relatively normal P granule staining in the germlines. (B'-E') sterile *prg-1,*
769 *nrde-4, hrde-1*, and *nrde-1* germ cell P granules.
770
771
772

	Total Worms Scored	% Fertile	% Sterile
pgl-1 F1 at 25°C	91	22%	78%
pgl-1 F2 at 25°C	71	0%	100%

773
774 **Table S1: Related to Figure 3. Fertility of *pgl-1* mutants at 25°C.** P0 *pgl-1* mutants
775 were shifted to 25°C and fertility was measured for the F1 generation. Fertile F1 worms
776 were cloned and the fertility of the F2 generation was measured.
777
778

gene	***prg-1***	***nrde-1***	***nrde-4***
C06B3.7	4.331128036	1.732445354	2.669978253
dhs-26	3.88587979	3.752818032	1.793937273
bath-45	3.604851731	5.5002102	2.319444032
fbxb-97	3.555301139	3.002992933	3.278539846
irg-2	3.519633623	2.605415087	2.189754742
pud-4	3.226292885	2.956152303	4.407697185
pud-3	3.097392415	3.143142026	4.328678969
R09E10.2	2.745900789	5.100997358	4.251177196
Y53F4B.5	2.636725232	5.821227047	4.162462556
K08D12.6	2.631068263	2.955437046	0.277803871
R03H10.6	2.469258519	4.82098578	3.295830487
Y58A7A.5	2.397260966	1.795895	2.143861408
pud-1.1	2.299685196	2.556376909	3.17781014
T22B7.7	2.276777478	3.01143186	2.207919501
fbxa-224	2.248998131	4.226992478	1.979961678
swt-6	2.144598564	3.153313277	0.277029378
pud-2.1	2.119890425	2.781615959	2.880747229
pud-2.2	2.094123631	2.779337879	2.796566876
pud-1.2	2.080250623	2.559790088	3.000944771
catp-3	2.014970724	2.436698711	2.674464594

779
780 **Table S2: Related to Figure 4. Genes upregulated in late-generation *prg-1* mutants**
781 **and in sterile *nrde-1* and *nrde-4* mutant L4 larvae.**
782